Adsorption Free Energy of Single Amino Acids at the Rutile (110)/Water Interface Studied by Well-tempered Metadynamics

Azade YazdanYar[✦], Ulrich Aschauer[✦✦], Paul Bowen[✦*]

[✦]Department of Materials Science and Engineering, École Polytechnique Fédérale de Lausanne (EPFL), Lausanne 1015, Switzerland

[✦✦]Department of Chemistry and Biochemistry, University of Bern, Bern 3012, Switzerland

[*]Corresponding author: Paul Bowen (paul.bowen@epfl.ch)

Abstract

Single amino acids are present in blood plasma and are the building blocks of larger organic residues. Their interaction with surfaces is therefore crucial for biomedical applications in contact with blood. In this work, we use well-tempered metadynamics to study the adsorption of six amino acids, with non-polar (Ala and Leu), polar (Ser), positively charged (Arg and Lys) and negatively charged (Asp) side groups, on a negatively charged rutile (110) surface. The free energy of adsorption and the desorption barriers were determined for all amino acids under different adsorption conformations. When using the center of mass as the collective variable in well-tempered metadynamics, results for different amino acids were difficult to interpret due to different adsorption conformations on the surface overlapping in collective-variable space. After projecting onto separate collective variables for the backbone and the side group much clearer trends were observable. We show that, on the negatively charged surface of rutile, adsorption via the backbone occurs for all the amino acids irrespective of their side group. Adsorption driven via the side group only occurs for polar and charged side groups as opposed to the non-polar side groups. This points to the importance of interactions of the side group with

the strongly structured water layer rather than direct side group-surface interactions in determining the adsorption behavior.

1. Introduction

A thin oxide layer forms on titanium surfaces in the presence of air or water and it is reported that titanium biomaterials owe their biocompatibility to this oxide layer.[1–2] Inorganic surfaces, such as the titanium oxide layer on an implant, are covered by organic residues rapidly after their implantation in the body;[3–5] this can be favorable, in the case of biosensors and drug delivery systems;[6] or unfavorable, where interactions of the surface with ions and cells in the blood plasma, are hindered or prevented by this organic layer.[7]

Alongside experimental studies, computational work can provide insights on the underlying interaction mechanism. Molecular dynamics (MD) is one of the atomistic tools for performing computational studies on the interactions of molecules with surfaces.[8] In the equilibrium state, the system spends a significant portion of time within stable states,[9] which are local energy minima; rare events move the system from one stable state to the other.[10] Rare events occur very infrequently, due to the large energy barriers associated with them, but rather quickly once the barrier has been surpassed.[9] Observation of rare events in a standard molecular dynamics simulation is unlikely due to the still relatively short timescales accessible using current hardware and software.[10–13] Enhanced sampling methods, such as metadynamics, which we use here, bias the potential energy of the system to promote rare events. In metadynamics, Gaussians bias potentials are deposited in a space defined by one or a few collective variables (CVs).[14,15] The free energy can be derived from the deposited bias potential. In well-tempered metadynamics, which is one of the flavors of metadynamics, the deposition rate and bias height of these Gaussians decrease over the simulation time.[15,16]

Free amino acids represent one group of the many different biomolecules present in blood plasma[17] and they also build up larger organic residues such as peptides and proteins. Each amino acid consists of an amine group, a carboxyl group and a C_α which carries a hydrogen and a side group. The different side groups determine specific properties of amino acids. The small size of single amino acids makes their adsorption on a biomaterial surface more probable in the initial steps after implantation since they are expected to have faster kinetics compared to other (larger) biomolecules. Both experimental, as well as computational studies, have investigated the interaction of amino acids, in forms of single residues or sequences, with inorganic surfaces.[5,18–20] One of the main debates on this topic is whether the nature of such interaction is entirely electrostatic.[21] For example, adsorption of positively charged Lys to the titanium oxide with a negative charge is reported to be purely electrostatic at neutral pH.[22] Tentorio et al.[23] also observed that adsorption of Glu and Lys on amorphous titanium oxide nanoparticles always happens in the pH range where attractive Coulomb interaction exists but it also occasionally occurs in the pH range where the Coulomb interaction is repulsive. Notman et al.[19] compared the free energy of adsorption of methane (as the side chain of Ala) and methanol (as the side chain of Ser) on a quartz (100) surface using MD simulations. The free energy landscape for both moieties was similar, which is not expected as the two analogues are different (hydrophobic and polar, respectively). It was argued that the surface shields the hydrophobic residue (methane) from water, favoring the adsorption of the hydrophobic side chain on the quartz surface.

It is also still unclear whether the adsorption and interaction of a single amino acid with an inorganic surface is fully determined by the side group as it has been reported that in a zwitterion, the three potential binding groups (the amine group, the carboxyl group and the side group) compete to interact with the surface.[24,25] Schmidt studied the adsorption of different amino acids on the titanium oxide surface in different pH ranges.[25] Side groups from similar

categories (either non-polar, polar or charged) did not lead to similar adsorption behavior in the same pH range. While some non-polar amino acids adsorbed, others did not; the same behavior was observed for amino acids with polar side groups. However, amino acids with charged side groups (either positive or negative) always adsorbed on the surface.

In much computational work, the side group of the amino acids has often been studied because in a peptide chain, both the carboxyl group and amine group are engaged in peptide bonds with the neighboring amino acids and the interaction with the surface is mainly via the side group. Sultan et al.[26] used metadynamics to study the energetics of adsorption of the end part of the side chain (side chain analogues) of some amino acids on a rutile (110) surface with a surface charge density of -0.104 $C \cdot m^{-2}$. The non-polar side groups showed weak interaction with the surface while polar and charged side groups showed strong interaction; the side groups with an opposite charge to the surface adsorbing the strongest. For the polar and charged side chain analogues, they noted that the adsorption affinity increased in the order of Ser, Asp, Lys and Arg.

Brandt et al.[27] used umbrella sampling and metadynamics to look at the same question but on a non-hydroxylated and charge neutral rutile (100) surface. They looked at analogues of the side group for all 20 naturally occurring amino acids. The results of both methods were consistent and showed that polar and aromatic side groups had strong interactions with the surface while the non-polar (and non-aromatic) side groups had a weak affinity for the surface. Ser showed the strongest adsorption on the neutral rutile (100) surface and the free energy of adsorption increased in the order of Ala, Lys, Leu, Asp, Arg and Ser. They observed that positively charged Lys had a lower adsorption energy than the non-polar Leu; in fact, the authors mention that a trend for the charged side chains could not be generalized and the reason was that the strongly bound water on the surface shields the interactions between the surface and charged functional groups.

The free energy of adsorption of full amino acids using well-tempered metadynamics was studied on gold and silver surfaces.[28] While the adsorption behavior on a metallic substrate should be different from an inorganic surface, this study seems to be the closest study to ours, which considers the entire unit of amino acids and not just the side group. The authors observed different trends for different substrates. The adsorption free energy increased in the order of Leu, Ala, Lys, Asp, Arg and Ser on the silver substrate and in the order of Lys, Ala, Asp, Ser, Leu and Arg on the gold substrate.

Here, we use well-tempered metadynamics to investigate the adsorption conformation and behavior of different amino acids on a rutile surface from the viewpoint of the free energy. In considering the full amino acid, we would like to explore whether it is the side group or backbone which mainly drives the adsorption. Six amino acids are chosen to cover those with polar, non-polar and charged side groups. All the simulations are performed on the rutile (110) surface which carries a small negative charge. This surface has the lowest surface energy among other rutile surfaces and therefore, it is the most stable surface of rutile.[2] The well-tempered metadynamics simulations were carried out using a single collective variable (center of mass of the amino acid) followed by projection of the results onto two collective variables (center of mass of side group and backbone) for further analysis.

2. Simulation methods

Rutile surface. We study the (110) surface of rutile which is hydroxylated in presence of air or water. Two types of hydroxyl groups form on this surface: the bridging and the terminal hydroxyl.[29] Under physiological conditions (T∼37 ℃ and pH∼7.4), rutile is negatively charged with a surface charge density of approximately -0.1 $C \cdot m^{-2}$,[30,31] which stems from a partial deprotonation of bridging hydroxyl groups. Predota et al. showed that surface groups of rutile (surface Ti and the hydroxyl groups) are variable-charge atoms[29] and presented the partial

charges of these groups for different surface charge densities.[32] In the current work, we are concerned with the interaction of the amino acids with a single charged site on the surface, mainly to avoid complications related to the distribution of charged sites and the complexities which it can add to draw conclusions. Therefore, in this paper, we deprotonate only one bridging hydroxyl group on the rutile surface, which has 72 bridging and 72 terminal hydroxyl groups. This single deprotonated hydroxyl results in a surface charge density of -0.011 $C \cdot m^{-2}$ on our rutile (110) surface. The surface, the hydroxyl groups on the surface, and the single charge point on the surface are shown in figure S1. The partial charges of the surface groups at this surface charge density were calculated as explained in section SI-2 of the SI.

The surface dimensions of the rutile slab were 35×38 $Å^2$ with a thickness of 70 Å. A water layer with a thickness of 90 Å was added on one side of the solid slab in the z direction. The thickness of the solid slab was selected such that interactions between the upper and lower faces of the slab were avoided. Also, the thickness of the water layer assured bulk water properties when far from the solid-liquid interface or the liquid-vacuum surface. Periodic boundary conditions were applied in all directions. Along the z direction, the periodic images were separated from each other by a vacuum gap of 100 Å to prevent interaction between periodic images of the simulation box.

Amino Acids. Six amino acids were chosen (figure 1): alanine and leucine (Ala and Leu; both with a non-polar side group), serine (Ser; with a polar side group), aspartic acid (Asp; with a negatively charged side group), and arginine and lysine (Arg and Lys; both with positively charged side groups). The selection of amino acids was made in a way to consider amino acids with different side groups. Also, the amino acids were chosen similar to those present in the titanium-peptide binding sequence which consists of Arg-Lys-Leu-Pro-Asp-Ala amino acids. This hexapeptide has proven to have a high affinity for several surfaces, including titanium. In our choice of amino acids, we replaced the aromatic and non-polar Pro with the polar Ser. pK_a

and pK_b for all amino acids are less than 3.0 and more than 8.0.[33] In the pH range between these two values (e.g., the physiological pH of 7.4 at 37 °C), the carboxylate group is deprotonated and the amine group is protonated; amino acid in this state is called a zwitterion. The overall charge of the amino acid in the zwitterion state depends on the charge of the side group. The charging state of the side groups of each amino acid was chosen based on its pK. Therefore, with a pK of 12.48 and 10.53, for the amine side groups of Arg and Lys,[33,34] respectively, their side groups are protonated. With a pK of 3.65 for the carboxyl side group of Asp, [33,34] its side group is deprotonated. Ala, Leu and Ser have non-polar and polar side groups which do not protonate or deprotonate.

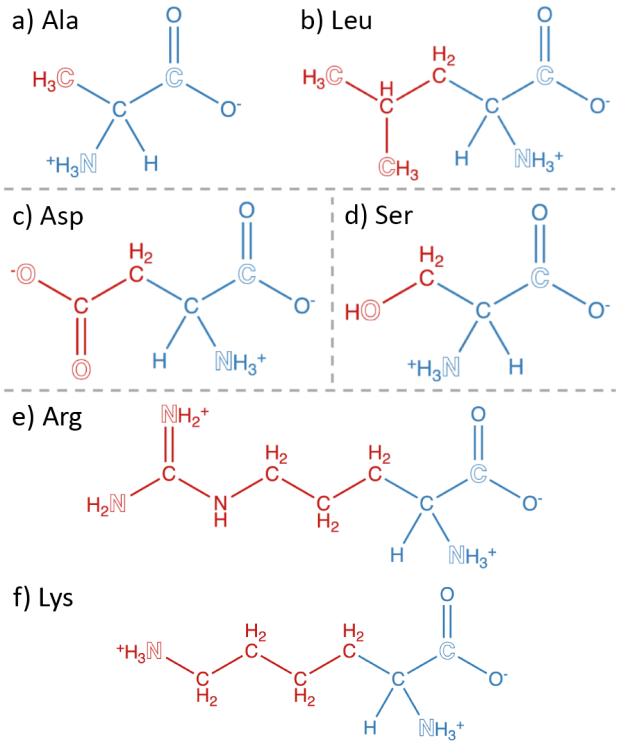

Figure 1. Amino acids studied in this work; a) alanine, b) leucine, c) aspartic acid, d) serine, e) arginine and f) lysine. Amino acids are labelled using their abbreviations in the figure. The atoms in blue are considered as the backbone and the atoms in red are the side group. Some of

the analyses, as stated in the text, are based on

the atoms shown with outline font.

Force fields. The classical force field developed by Predota et al.[29] was used to define interaction parameters of rutile. Water was modelled using the SPC/E model.[35] Rutile-water interactions were described by the parameters proposed by Predota et al.[29] which are based on previous *ab initio* studies.[36] The force field input files for the amino acids were prepared by the DL_FIELD package.[37] The CHARMM force field[38] was used in this package to obtain the interaction parameters. Parameters for cross-interactions between water and the amino acids, and between rutile and the amino acids were all obtained using the mixing rules of Lorentz-Berthelot.[39] Since the parameters in the Lennard-Jones form are required to use these mixing rules, fitting of the Lennard-Jones form to the force field parameters of rutile to the Buckingham form was carried out (see SI-3). It should be noted that for describing rutile, we used the force field developed by Predota et al.[29] in the Buckingham form and the Lennard-Jones parameters were used only for rutile-amino acid interactions. The cutoff for the short-range van der Waals interactions as well as the real space part of the electrostatic calculations was 12 Å. Long-range electrostatics were treated by an Ewald summation. A Nosé-Hoover thermostat with a relaxation time of 0.5 ps was used to impose a temperature of 37 ℃ in the NVT ensemble. The equations of motion were integrated with a time step of 0.7 fs. The integration algorithm was Verlet leapfrog.

Simulation details. Well-tempered metadynamics simulations[16] were performed using DL_Classic v1.9[40] with the Plumed plugin v2.2.2.[41] Gaussian hills with an initial height of 1 $kJ{\cdot}mol^{-1}$ and a width of 0.5 Å were deposited every 2,000 time steps (1.4 ps) with a bias factor of 15. Before production runs, each system was equilibrated for 200-250 ps during which the C_α atom of the amino acid was kept fixed at a distance of 15 Å from the surface. All atoms of

the rutile slab, except the hydroxyl groups on the surface, were kept frozen during the equilibration and production runs to speed up the computation. The perpendicular distance of the center of mass of the amino acids from the surface was considered as the collective variable (CV_{COM}) and it was limited to a distance of 12 Å from the surface in the z direction. The surface position was defined to be the average z component of the oxygen atoms of all the hydroxyl groups. In the XY plane, the center of mass of the amino acid was confined to move within a radius of 4 Å around the charge point on the surface (figure S1).

To be able to better differentiate the role of the backbone and the side group of an amino acid in its adsorption behavior, we projected the results obtained in the CV_{COM} space into a two-dimensional space that allows us to differentiate between adsorption of the backbone and the side chain. The validity of this so-called reweighting approach,[42] in particular in combination with well-tempered metadynamics, was previously shown for projections onto two dihedral angles after having biased the dynamics of only a third dihedral in an alanine dipeptide.[42] Plumed analysis tools were used for post-processing. The 'reweight_metad' functionality of Plumed was first used cancel out the bias applied to the system due to the usage of CV_{COM}. This functionality implements the Tiwary-Parrinello reweighting method[42] to an already biased trajectory. Then, the 'histogram' functionality was used to accumulate the average probability density of the two new collective variables. Finally, 'convert_to_fes' was used to obtain the free energy profile.

The two-dimensional space we project into is spanned by the collective variables $CV_{Backbone}$ and CV_{Side}. Both collective variables represent the distance from the surface in the z direction for the center of mass of a part of the amino acid. The $CV_{Backbone}$ takes into account the amine group, the carboxyl group, the C_α and its hydrogen. The CV_{Side} includes the rest of the amino acid which we refer to as the side group. The groups of atoms considered for the backbone and the side group are shown in figure 1 in blue and red, respectively. The free energy landscape as

a function of these two collective variables helped us to detect favorable adsorption conformations. We will also be able to see if an amino acid prefers to approach the surface mainly via the backbone, the side group or both.

All simulations were carried out for 20 ns, corresponding to 31-44 days per calculation on our available HPC resources. Using the block analysis method, the average error of the calculations was estimated for different block sizes. Figure S3 shows the error corresponding to each amino acid as the block size increases. As the convergence of the error value can be a proper criterion for sufficient sampling, we can say that the simulation length is acceptable. The estimated error associated with our calculations (performing well-tempered metadynamics using the CV_{COM}) is less than 1.6 $kJ.mol^{-1}$.

3. Results and Discussion

3.1.Water-Surface interactions and adsorption mode of amino acids

It has been shown that close to rutile surfaces, independent of surface charge, water is orientated in a few layers with a higher density than bulk water.[26,29,43] The water density in the normal direction to the surface is plotted in figure S4. As it can be seen in this figure, there are high-density water layers at distances of 2.35 and 4.6 Å from the surface, which is in agreement with previous studies.[29,44,45] We define direct binding when a group binds directly to the surface without the presence of intermediate water molecules. During this binding mode, the binding group has to lose some of its associated water molecules. Unlike direct binding, indirect binding involves the presence of water molecules between the binding group and the surface. Many studies have emphasized the competition between water and the adsorbate during the adsorption of organic residues on the surface. In many cases, the indirect binding can have a long residence time and can be the primary binding mode of the adsorbate.[27,46,47] The stability or residence time of a bound configuration depends on the energy required to distort the bond. If such energy

is not negligible, the bond will have a longer residence time. For the sake of simplicity, in our study we have considered the adsorption mode to be indirect if the bonding distance from the surface is further than the water layer closest to the surface (at 2.35 Å) since in such a case, water molecules are present between the adsorbent and the surface. We consider the bonding mode to be direct if the adsorption distance from the surface is closer than this water layer to the surface mainly because in such a case, the adsorbent has a high affinity for the surface which has allowed it to pass the closest water layer to the surface, reach the surface and have a direct interaction with it.

The distance of the main atom of each group (outline fonts in figure 1) from the surface is shown in figure 2 (for those with two end atoms in the side group, the average value is plotted); we also present some atomic snapshots over the simulation time in this figure. Close observation of this figure for different amino acids reveals that in the adsorbed state, most of the time, one of the potential binding groups is closer to the surface than the first water layer (shown as the horizontal dashed line in figure 2) meaning that the adsorption is driven by direct binding with at least one of the groups. For the cases where the adsorption is mainly via the carboxyl group (e.g., figure 2-b in the time interval of 16-18 ns) or a negatively charged side group (figure 2-c in the time interval of 12-12.5 ns), the repulsive electrostatics between the negative charge point on the surface and the negatively charged binding group of the amino acid (the carboxyl group in the backbone or the side group of Asp) causes the adsorption to take place slightly farther from the surface (figure 2-c-ii). Nonetheless, since there is no water molecule between the binding group and the surface, this adsorption mode is still considered to be direct (figure 2-b-ii). In fact, based on figure 2, we do not observe any indirect yet stable binding of the amino acid to the surface, i.e., there is no clear stable adsorption in which the distance of the binding group from the surface is more than the first water layer while water molecules can be seen in the atomic snapshot between the binding group and the surface.

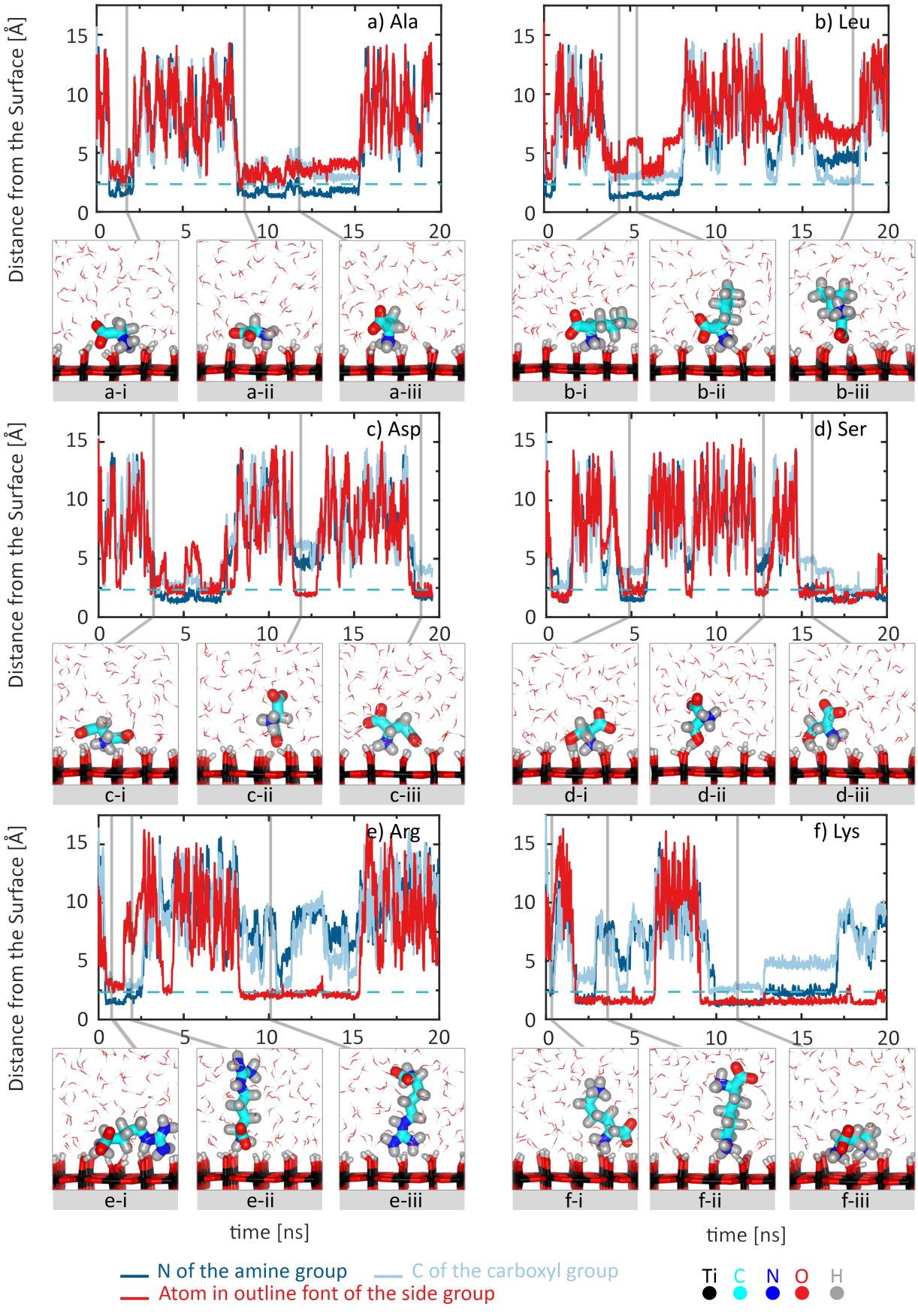
a) Ala
b) Leu
c) Asp
d) Ser
e) Arg
f) Lys
Distance from the Surface [Å]
time [ns]
a-i
a-ii
a-iii
b-i
b-ii
b-iii
c-i
c-ii
c-iii
d-i
d-ii
d-iii
e-i
e-ii
e-iii
f-i
f-ii
f-iii
N of the amine group
C of the carboxyl group
Atom in outline font of the side group
Ti
C
N
O
H

Figure 2. Distance from the surface of outlined atoms of figure 1, for a) Ala, b) Leu, c) Asp, d) Ser e) Arg and f) Lys. For Leu, Asp and Arg the red plot corresponds to the average of two outlined atoms of the side group in figure 1. The dashed horizontal line shows the position of the first water layer. Atomistic snapshots (labelled by i, ii and iii) were visualized by Vesta[48] and correspond to the time points shown by grey lines.

3.2.Free energy profile using CV_{COM}

The free energy as a function of the center of mass of the amino acid from the surface (collective variable CV_{COM}), is shown in figure 3. This CV allows the amino acid to approach the surface in different orientations and conformations of the backbone and the side group. In previous studies by other groups, the center of mass was used to examine the energetics of the adsorption;[26,27] since these studies investigate only side group analogues of the amino acid, the use of this collective variable can be sufficient in obtaining proper free energy profiles of the adsorption. Here, however, we observe that using only CV_{COM} fails to provide sufficient details with respect to the adsorption behavior; for example, in figure 3, it is unclear why Ala and Ser have similar energy landscapes and what causes a single-well landscape for these two amino acids but not for the others. Even Arg and Lys, which have similar positively charged side groups, show different energy states in their multi-well energy profiles. Consequently, we use the so-called reweighting method[42] so that we could extract more details from the atomistic trajectories.

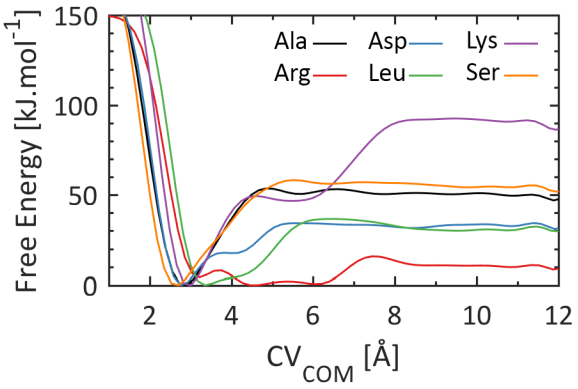

Figure 3. Free energy profile as a function of the CV_{COM} (distance of the center of mass of amino acid from the surface).

3.3.Free energy profile after reweighting

The nature of the adsorption mode can be further understood by reconstructing the free energy of adsorption with respect to the backbone and the side group using a reweighting method[42] as explained in the following. It is important to note that increasing the dimensionality of the CV space during reweighting can lead to limitations and that directly performing well-tempered metadynamics using $CV_{Backbone}$ and CV_{Side} would be preferable, although computationally much more intensive. We hence use reweighting here as a means of projecting results of CV_{COM} into the two-dimensional space of $CV_{Backbone}$ and CV_{Side}. It should also be noted that we tried reweighting using two separate collective variables for the amine and the carboxyl group but the small and almost constant distance between these two groups makes these two collective variables correlated. As the collective variables in metadynamics should be independent, the amine and carboxyl groups, along with C_α and its hydrogen, were considered as the backbone group while the remaining part of the amino acid was considered as the side group (see blue and red coloring in figure 1, respectively).

The free energy landscape as a function of the $CV_{Backbone}$ and the CV_{Side} is shown in figure 4. All the amino acids show an energy minimum where both the $CV_{Backbone}$ and the CV_{Side} are

small (point A). In such a conformation, both the backbone and the side group are involved in the adsorption of the amino acid on the surface. An energy minimum at point S (small CV_{Side} and large $CV_{Backbone}$) represents adsorption of the amino acid via only its side group while an energy minimum at point B (small $CV_{Backbone}$ and large CV_{Side}) represents the adsorption of the amino acid only via the backbone.

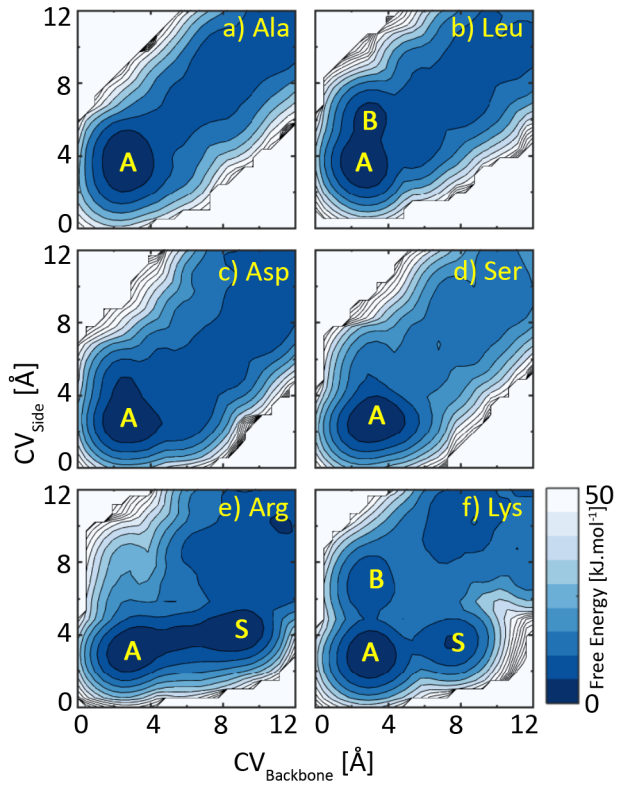

Figure 4. Free energy landscape as a function of $CV_{Backbone}$ and CV_{Side}, which are the distance of the center of mass of the backbone and the side group from the surface, respectively for a) Ala, b) Leu, c) Asp, d) Ser e) Arg and f) Lys. Points A, B and S are adsorption via A: both backbone and side group, B: backbone and S: side group.

The free energy map in 2D (figure 4) can be further clarified by using the radius of gyration (R_g) of the individual amino acids (figure S5-a). Here, we discuss the adsorption behavior of amino acids in increasing order of R_g which is Ala, Ser, Asp, Leu, Lys and Arg; the values are reported in table 1 and are obtained from performing molecular dynamics simulations on a box of water containing single amino acids (figure S5-b). Ala, as the amino acid with the smallest R_g, shows a single energy well at point A in which the adsorption seems to be via both the backbone and the side group (figure 2-a-i and ii). However, close observation of figure 2-a reveals that in the adsorbed state, most of the time, the adsorption is directly driven by the amine group (figure 2-a-iii). We can also see in figure 4-a that the energy minimum of Ala at point A is extended vertically, which shows that in this adsorption conformation, the side group is further from the surface than the backbone. So, the dominant adsorption mode of Ala is rather with the amine group in the backbone than the backbone and side groups together.

Table 1. Radius of gyration, adsorption energy on the surface and normalized desorption rates for the amino acids.

Amino acid	R_g [Å]	ΔE_{ads} [kJ·mol^{-1}]	r_{des}/A
Ala	1.87 ± 0.02	50.14	3.53 * 10^{-9}
Leu	2.40 ± 0.03	30.92	6.13 * 10^{-6}
Asp	2.08 ± 0.02	32.83	2.92 * 10^{-6}
Ser	1.99 ± 0.03	54.92	5.52 * 10^{-10}
Arg	3.18 ± 0.10	< 4 Å: 3.89 4-8 Å: 10.52	2.21 * 10^{-1} 1.68 * 10^{-2}
Lys	2.90 ± 0.07	91.06	4.46 * 10^{-16}

Ser has a slightly larger R_g compared to Ala and as seen in figure 2-d-i, ii, iii, it can adsorb either via the side group or the side group and the backbone. The fact that we observe only one energy minimum for Ser at point A, similar to Ala, is due to its small size, which does not allow

us to resolve other possible energy minima such as B and S. For Asp, we observe that the energy minimum at point A is extended both vertically towards the region of adsorption via the backbone and horizontally towards the region of adsorption via the side group. However, it seems that the size of Asp is still too small for the energy minimum to be separated from each other. In summary, for smaller amino acids (Ala, Asp and Ser), in our setup, the small R_g prevents the formation of a noticeable energy minimum other than point A even if either of the side group or the backbone are mainly driving the adsorption.

Leu exhibits a similar behavior to Ala; in the adsorbed state, the adsorption is direct via the backbone (figure 2-b-i, ii and iii). The larger size of Leu allows the formation of the energy minimum at point B. Arg and Lys exhibit several energy minima, as well. One would expect similar free energy landscapes for Arg and Lys due to their similarity in having a positively charged side group but the minimum at point B does not appear for Arg. One explanation could be that since Arg has a larger R_g than Lys (figure S5), in cases where the backbone is adsorbed on the surface, the larger R_g of Arg (or eventually its longer chain) provides it with more flexibility, which makes it possible for the side group to undergo conformational changes and find a second adsorption site on the surface (figure 2-e-i). Consequently, we believe that the adsorption via the backbone generally leads to the concurrent adsorption of the side group on the surface and so, point B is not present for Arg. Nevertheless, figure 2-e-ii represents adsorption of Arg via the backbone, which is transient as it eventually is accompanied by the adsorption of the side group. For Lys, on the other hand, the side group is slightly shorter which reduces its flexibility compared to Arg. As a result, we observe adsorption via a single group (backbone or side group) and both these groups for this amino acid (figure 2-f-i, ii, iii), which is reflected by the presence of three distinct energy minima.

Figure 4 also helps us to understand different free energy landscapes, which were observed in figure 3. As already mentioned, we see that for small amino acids, separate energy minima

do not form and consequently, Ala, Ser and Asp show one major energy well in figure 3. Similarly, we can now explain why the other three amino acids show multiple or broader energy wells in figure 3. Thus, we show that using only CV_{COM} is not sufficient in studying the detailed adsorption behavior of amino acids especially with a larger size.

To compare the adsorption conformation of different amino acids more quantitatively and discuss the adsorption conformations in more details, we replot figure 4 in 1D, where the free energy is projected along each collective variable (figure 5). In figure 5, the deep well at distances less than 5 Å from the surface, for all amino acids, points to the energy minimum at point A in figure 4. For Ala, Asp and Ser, free energy along the $CV_{Backbone}$ is very similar to the free energy along the CV_{Side} which is due to their small R_g which causes them to possess one major energy well (figures 3 and 4). For Ala, we observe that the deep energy well of the backbone (figure 5-a in blue) is closer to the surface than that of the side group (figure 5-a in red) which is the other way around for Ser. This again shows that in the adsorbed state, the backbone is closer to the surface than the side group for Ala, but the side group is closer than the backbone for Ser (figure 2-a-iii and 2-d-ii). This is attributed to the non-polar and polar nature of the Ala and Ser side group, respectively.

The energy wells along the collective variables are labeled in figure 5 in accordance with figure 4. As mentioned before, Arg is slightly longer than Lys and this can be seen in figure 5 where the distance of the energy minimum at point S for Lys is closer to the surface compared to Arg. For Lys side-group adsorption is more favorable than backbone adsorption with an energy difference of 1.72 $kJ \cdot mol^{-1}$ and is less favorable than the double adsorption with an energy difference of 7.87 $kJ \cdot mol^{-1}$.

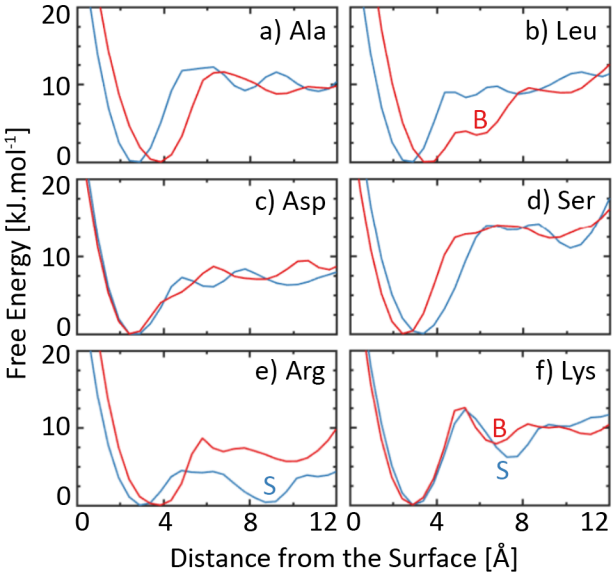

Figure 5. Free energy profile projected along only one collective variable ($CV_{Backbone}$: blue: and CV_{Side}: red). 'B' is the energy minimum along CV_{Side} and 'S' is the energy minimum along $CV_{Backbone}$, for a) Ala, b) Leu, c) Asp, d) Ser e) Arg and f) Lys.

3.4. Desorption rate from the surface

In table 1, we also report the energy gain of amino acids during the adsorption (ΔE_{ads}), which is the difference between the solvated state (distances larger than 8 Å from the surface) and the global energy minimum (normalized to 0 kJ·mol^{-1} for all the amino acids) in figure 3. Only for Arg, adsorption and desorption seem to be separated by an intermediate energy barrier close to 4 Å (figure 3). Therefore, for Arg, we mention the depth of energy well at two regions: before 4 Å and between 4 and 8 Å. From table 1, we see that ΔE_{ads} for Ala and Ser is similar. For Asp, we only observe an energy minimum at point A in figure 4. However, ΔE_{ads} of Asp on the surface is smaller than for Ala and Ser, the reason for which we think is the repulsive

electrostatics between the charge point on the surface and the side group of Asp, which make the adsorption less favorable.

The smaller ΔE_{ads} of Leu compared to Ala, which both have non-polar side groups, might be due to the fact that the Ala side group contains one methyl group (CH_3) while Leu contains two. The non-polar side groups might be trying to avoid the well-defined water structure close to the rutile surface more in the case of Leu with two methyl groups compared to Ala. Even though both Arg and Lys have a side group with a +1e charge, they are different in their functional groups; Arg ends with two NH_2 groups while Lys has one NH_3 group (figure 1). While the Lennard-Jones interactions, which describe the interaction of these group with other atoms, are similar for both Arg and Lys, the nitrogen and hydrogen atoms are more negative and positive, respectively, in Arg compared to Lys.

ΔE_{ads} for Lys is larger than for all other amino acids. Since this amino acid has a stable adsorption via the side group or via the backbone, the addition of these two results in a larger energy gain when we study the adsorption using CV_{COM}.

Given the barrierless adsorption profiles, we can use ΔE_{ads} and the transition state theory to have an insight into the desorption rate of amino acids from the surface. The rate constant of a transition with an activation energy of ΔE can be described as $A \exp(^{-\Delta E}/_{k_B T})$; where A is a pre-exponential factor describing the attempt rate, and k_B and T are the Boltzmann constant and temperature, respectively.[49] The coefficient A is the temperature-dependent rate prefactor and is typically in the range of 10^{13}-10^{14} [1/s]. In order to avoid the problem of choosing a specific value for the pre-exponential factor, we present the desorption rate of amino acids from the surface, normalized by A, in table 1 which is unit-less. If we were to consider a value for A, it will be the same value for all rate constants of amino acids.

3.5.Amino acid-Water interactions

During the adsorption process, the binding groups of the amino acids have to lose some of their associated water molecules. To see which amino acids have a stronger association with water, we can look at the radial distribution function of the amine, carboxyl and side groups with respect to the oxygen of water. For this analysis, we performed unbiased molecular dynamics simulation of the individual amino acids solvated in water. The radial distribution functions between the amine group and the carboxyl group with the oxygen of water (shown in figure S6) are similar for all the amino acids. Figure 6 shows the radial distribution function between the side group (atoms with outline fonts in figure 1) and oxygen of water. For Arg, Asp and Leu, the radial distribution function is plotted only for one of the atoms of the side group shown with outline font (figure 1). The absence of a significant peak for Ala and Leu, at distances closer than 4 Å, is due to their hydrophobic nature. The polar and charged amino acids show strong interaction with water molecules. Asp shows the strongest interaction with water molecules which is due to the side group consisting of bare oxygens while in Arg, Lys and Ser functional groups, the oxygens are bonded to hydrogen atoms. The difficulty for the side group to lose some of its associated water is related to the energy difference between the maximum and the local minimum in figure 5 (on the CV_{Side} plot). This increases in the order of Ser, Arg, Lys, Asp which is in agreement with figure 6. This can help us also explain the trend of ΔE_{ads} in table 1 where, we see that for example, the adsorption of Asp on the surface is accompanied with a larger energy compared to that of Arg.

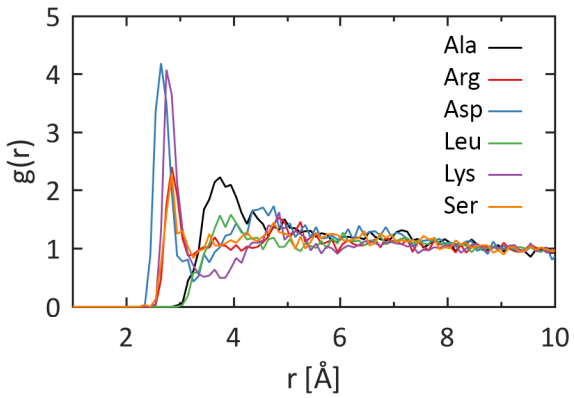

Figure 6. Radial distribution function of the side group with water (OW).

3.6. Summary

As mentioned in the introduction, to the knowledge of authors, most of the computational work on the adsorption of amino acids on surfaces only considers the side group. Thus, it is difficult to directly compare our results with those in the literature. Nevertheless, in general based on the literature, it seems that on a charge neutral surface, Ser has a high affinity for the surface and on a charged surface, amino acids with an opposite charge to the surface show higher affinity. The non-polar amino acids show a low affinity for surfaces. Our results are in agreement with these observations thus validating the use of the reweighting method for our system. Using this method, we were able to extract more information from our well-tempered metadynamics simulations and to explain the free energy changes associated with the adsorption of amino acids on the rutile (110) surface.

Compared to the results of Sultan et al.[26] and Brandt et al.[27] (the latter being for the (100) surface and not the (110) surface), which show that non-polar side chain analogues have a very weak or even repulsive interaction with the surface, we argue that when considering the entire amino acid in its zwitterion state, the adsorption can occur even for these amino acids, which is in agreement with the work of Tran et al.[24] where the adsorption of Ala on the titanium oxide

surface was observed. To address the questions posed in the introduction, on whether the interaction of amino acids with the surface is thoroughly electrostatic, or is driven only via the side group, we believe that the electrostatic interactions are important since they can lead to the adsorption of the backbone of a zwitterion even if the side group is non-polar. We also show that the adsorption of a zwitterion on a charged surface can be via the backbone, as it contains charged amine and carboxyl groups. There is a competitive adsorption between water and the amino acids on the surface. The high hydrophilicity of the surface leads to strongly structured water layers to an extent where only polar and charged side groups but not non-polar side groups are able to traverse the water layer and directly bind to the surface.

4. Conclusion

We have studied the adsorption of six amino acids – covering polar, non-polar and charged side groups – onto a negatively charged rutile (110) surface using metadynamics in the presence of water. Our metadynamics simulations reveal that if we consider only the distance of the center of mass of an amino acid to the surface as the collective variable, it does not provide sufficient details on the adsorption conformation to allow us to differentiate between different adsorption modes. Using the reweighting method, we project the free energy into a space of two collective variables, the distances of the backbone (carboxyl, amine, C_α and its hydrogen) and the side group to the surface, and show that the adsorption in the vicinity of a negative charge point can always happen via the backbone (mainly the amine group) irrespective of the type of the side group. This explains why adsorption of amino acids on surfaces was previously reported, even for repulsive or weak interaction of the side group with the surface. The adsorption of amino acids with non-polar side groups is shown to be mainly via their backbone. For polar and charged amino acids, both the backbone and the side group can engage in the binding process and adsorption is robust when the side group has an opposite charge to the surface. Since the

rutile surface is hydrophilic, a potential binding site has to lose the strongly orientated water molecules close to the surface to be able to directly bond the amino acid. We observe that only direct binding is stable and no indirect yet stable binding was observed. From the computed energy profiles, relative adsorption strengths and adsorption-desorption kinetics can be estimated via transition state theory to further enhance our understanding of the kinetics of amino acid interactions with surfaces. Experimental studies are currently being undertaken in our laboratory to further validate our results using zeta potential measurements and TGA by obtaining adsorption isotherms.

Conflict of interest

None.

Supporting Information

Atomic partial charges of the rutile surface; Lennard-Jones force field parameters for rutile; Error estimation; Water density close to the surface; Radius of gyration of amino acids; Radial distribution functions with water.

Acknowledgement

This work was supported by the Swiss National Science Foundation [SNSF BioCompSurf 513468]. Scientific IT and Application Support Center (SCITAS) of EPFL were used for the CPU time.

References

1. Liu, X.; Chu, P.; Ding, C. Surface Modification of Titanium, Titanium Alloys, and Related Materials for Biomedical Applications. Mater. Sci. Eng. R. 2004, 47, 49–121 DOI: 10.1016/j.mser.2004.11.001.
2. Diebold, U. The Surface Science of Titanium Dioxide. Surf. Sci. Rep. 2003, 48, 53–229 DOI: 10.1016/S0167-5729(02)00100-0.
3. Kasemo, B.; Gold, J. Implant Surfaces and Interface Processes. Adv. Dent. Res. 1999, 13, 8–20 10.1177/08959374990130011901.
4. Kasemo, B. Biological Surface Science. Surf. Sci. 2002, 500, 656–677 DOI: 10.1016/S1359-0286(98)80006-5.
5. Silva-Bermudez, P.; Rodil, S. E. An Overview of Protein Adsorption on Metal Oxide Coatings for Biomedical Implants. Surf. Coat. Technol. 2013, 233, 147–158 DOI: 10.1016/j.surfcoat.2013.04.028.
6. Gertler, G.; Fleminger, G.; Rapaport, H. Characterizing the Adsorption of Peptides to TiO_2 in Aqueous Solutions by Liquid Chromatography. Langmuir 2010, 26, 6457–6463 DOI: 10.1021/la903490v.
7. Zhao, W.; Lemaitre, J.; Bowen, P. A Comparative Study of Simulated Body Fluids in the Presence of Proteins. Acta Biomater. 2017, 53, 506–514 DOI: 10.1016/j.actbio.2017.02.006.
8. Yazdanyar, A.; Aschauer, U.; Bowen, P. Interaction of biologically relevant ions and organic molecules with titanium oxide (rutile) surfaces: A review on molecular dynamics studies. Colloids Surf B Biointerfaces 2018, 161, 563–577 DOI: 10.1016/j.colsurfb.2017.11.004.
9. Dellago, C.; Bolhuis, P. G.; Geissler, P. L. Transition Path Sampling Methods. Lect. Notes Phys. 2006, 703, 349–391 DOI: 10.1007/3-540-35273-2_10.
10. Latour, R. A. Molecular Simulation of Protein-Surface Interactions: Benefits, Problems, Solutions, and Future Directions (Review). Biointerphases 2008, 3, FC2-FC12 DOI: 10.1116/1.2965132.
11. Valsson, O.; Tiwary, P.; Parrinello, M. Enhancing Important Fluctuations: Rare Events and Metadynamics from a Conceptual Viewpoint. Annu. Rev. Phys. Chem. 2016, 67, 159–184 DOI: 10.1146/annurev-physchem-040215-112229.
12. Sutto, L.; Marsili, S.; Gervasio, F. L. G. New Advances in Metadynamics. WIREs Comput. Mol. Sci. 2012, 2012, 2, 771–779 DOI: 10.1002/wcms.1103.

13. Deighan, M.; Pfaendtner, J. Exhaustively Sampling Peptide Adsorption with Metadynamics. Langmuir 2013, 29, 7999–8009 DOI: 10.1021/la4010664.
14. Laio, A.; Gervasio, F. L. Metadynamics: A Method to Simulate Rare Events and Reconstruct the Free Energy in Biophysics, Chemistry and Material Science. Rep. Prog. Phys. 2008, 71, 126601–1:22 DOI: 10.1088/0034-4885/71/12/126601.
15. Barducci, A.; Bonomi, M.; Parrinello, M. Metadynamics. Comput. Mol. Sci. 2011, 1, 826–843 DOI: 10.1002/wcms.31.
16. Barducci, A.; Bussi, G.; Parrinello, M. Well-Tempered Metadynamics: A Smoothly Converging and Tunable Free-Energy Method. Phys. Rev. Lett. 2008, 100, 020603–1:4.
17. Stein, W.; Moore S. The Free Amino Acids of Human Blood Plasma. J. Biol. Chem. 1954, 211, 915–926.
18. Kubiak-Ossowska, K.; Tokarczyk, K.; Jachimska, B.; Mulheran, P. A. Bovine Serum Albumin Adsorption at a Silica Surface Explored by Simulation and Experiment. J. Phys. Chem. B 2017, 121, 3975−3986 DOI: 10.1021/acs.jpcb.7b01637.
19. Notman, R.; Walsh, T. R. Molecular Dynamics Studies of the Interactions of Water and Amino Acid Analogues with Quartz Surfaces. Langmuir 2009, 25, 1638–1644 DOI: 10.1021/la803324x.
20. Hook, F.; Voros, J.; Rodahl, M.; Boni, P.; Ramsden, J. J.; Textor, M.; Spencer, N. D.; Tengvall, P.; Gold, J.; Kasemo, B. A Comparative Study of Protein Adsorption on Titanium Oxide Surfaces Using in Situ Ellipsometry, Optical Waveguide Lightmode Spectroscopy, and Quartz Crystal Microbalance/Dissipation. Colloids Surf. B Biointerfaces 2002, 24, 155–170 DOI: 10.1016/S0927-7765(01)00236-3.
21. Roddick-Lanzilotta, A.; McQuillan, A. J. An in Situ Infrared Spectroscopic Study of Glutamic Acid and of Aspartic Acid Adsorbed on TiO_2: Implications for the Biocompatibility of Titanium. Colloid Interface Sci. 2000, 227, 48–54 DOI: 10.1006/jcis.2000.6864.
22. Roddick-Lanzilotta, A. D.; Connor, P. A.; Mcquillan, A. J. An In Situ Infrared Spectroscopic Study of the Adsorption of Lysine to TiO_2 from an Aqueous Solution. Langmuir 1998, 14, 6479–6484 DOI: 10.1021/la980425n.
23. Tentorio, A.; Canova, L. Adsorption of Alpha-Amino Acids on Spherical TiO_2 Particles. Colloids Surf. 1989, 39, 311–319 DOI: 10.1016/0166-6622(89)80282-3.
24. Tran, T. H.; Nosaka, A. Y.; Nosaka, Y. Adsorption and Photocatalytic Decomposition of Amino Acids in TiO_2 Photocatalytic Systems. J. Phys. Chem. B 2006, 110, 25525–25531 DOI: 10.1021/jp065255z.

25. Schmidt, M. X-Ray Photoelectron Spectroscopy Studies on Adsorption of Amino Acids from Aqueous Solutions onto Oxidised Titanium Surfaces. Arch. Orthop. Trauma Surg. 2001, 121, 403–410.
26. Sultan, A. M.; Hughes, Z. E.; Walsh, T. R. Binding Affinities of Amino Acid Analogues at the Charged Aqueous Titania Interface: Implications for Titania-Binding Peptides. Langmuir 2014, 30, 13321−13329 DOI: 10.1021/la503312d.
27. Brandt, E. G.; Lyubartsev, A. P. Molecular Dynamics Simulations of Adsorption of Amino Acid Side Chain Analogues and a Titanium Binding Peptide on the TiO_2 (100) Surface. J. Phys. Chem. C 2015, 119, 18126–18139 DOI: 10.1021/acs.jpcc.5b02670.
28. Palafox-Hernandez, J. P.; Tang, Z.; Hughes, Z. E.; Li, Y.; Swihart, M. T.; Prasad, P. N.; Walsh, T. R.; Knecht, M. R. Comparative Study of Materials-Binding Peptide Interactions with Gold and Silver Surfaces and Nanostructures: A Thermodynamic Basis for Biological Selectivity of Inorganic Materials. Chem. Mater. 2014, 26, 4960−4969 DOI: 10.1021/cm501529u.
29. Predota, M.; Bandura, A. V.; Cummings, P. T.; Kubicki, J. D.; Wesolowski, D. J.; Chialvo, A. A.; Machesky, M. L.; Pr, M. Electric Double Layer at the Rutile (110) Surface . 1 . Structure of Surfaces and Interfacial Water from Molecular Dynamics by Use of ab Initio Potentials. J. Phys. Chem. B 2004, 108, 12049–12060 DOI: 10.1021/jp037197c.
30. Machesky, M. L.; Wesolowski, D. J.; Palmer, D. A.; Ridley, M. K.; Bénézeth, P.; Lvov, S. N.; Fedkin, M. V. Chapter 12 Ion Adsorption into the Hydrothermal Regime: Experimental and Modeling Approaches. Interface Sci. Technol. 2006, 11, 324–358 DOI: 10.1016/S1573-4285(06)80056-6.
31. Takahashi, K.; Satoshi, F. Cleanability of Titanium and Stainless Steel Particles in Relation to Surface Charge Aspects. Biocontrol Sci. 2008, 13, 9–16 DOI: 10.4265/bio.13.9.
32. Predota, M.; Machesky, M. L.; Wesolowski, D. J.; Cummings, P. T. Electric double layer at the rutile (110) surface. 4. effect of temperature and pH on the adsorption and dynamics of ions. J. Phys. Chem. C 2013, 117, 22852–22866 DOI: 10.1021/jp407124p.
33. Lundblad, R.; Macdonald, F. Handbook of Biochemistry and Molecular Biology, Fourth Edition. CRC Press 2010.
34. Harris, T. K.; Turner, G. J. Structural Basis of Perturbed pK a Values of Catalytic Groups in Enzyme Active Sites. IUBMB Life 2002, 53, 85–98 DOI: 10.1080/10399710290038972.
35. Berendsen, H. J. C.; Grigera, J. R.; Straatsma, T. P. The Missing Term in Effective Pair Potentials. J. Phys. Chem. 1987, 91, 6269–6271 DOI: 10.1021/j100308a038.

36. Bandura, A. V; Kubicki, J. D. Derivation of Force Field Parameters for TiO_2-H_2O Systems from ab Initio Calculations. J. Phys. Chem. B 2003, 107, 11072–11081 DOI: 10.1021/jp034093t.
37. Yong, C. W. Descriptions and Implementations of DL_F Notation: A Natural Chemical Expression System of Atom Types for Molecular Simulations. J. Chem. Inf. Model 2016, 56, 1405–1409.
38. MacKarell, A. D.; Bashford, D.; Bellott, M.; Dunbrack, R. L.; Evanseck, J. D.; Field, M. J.; Fischer, S.; Gao, J.; Guo, H.; Ha, S.; et al. All-Atom Empirical Potential for Molecular Modeling and Dynamics Studies of Proteins. J. Phys. Chem. B 1998, 102, 3586–3616 DOI: 10.1021/jp973084f.
39. Allen, M. P.; Tildesley, D. J. Computer Simulation of Liquids. Clarendon Press 1987.
40. Smith, W.; Forester, T. R.; Todorov, I. T. The DL_POLY Classic User Manual. SFTC Daresbury Laboratory; 2012.
41. Tribello, G. A.; Bonomi, M.; Branduardi, D.; Camilloni, C.; Bussio, G. PLUMED 2: New Feathers for an Old Bird. Comput. Phys. Commun. 2014, 185, 604–613 DOI: 10.1016/j.cpc.2013.09.018.
42. Tiwary, P.; Parrinello, M. A Time-Independent Free Energy Estimator for Metadynamics. J. Phys. Chem. B 2015, 119, 736–742 DOI: 10.1021/jp504920s.
43. Skelton, A. A.; Walsh, T. R. Interaction of Liquid Water with the Rutile TiO_2 (110) Surface. Mol. Simul. 2007, 33, 379–389 DOI: 10.1080/17441690701191693.
44. Kavathekar, R. S.; Dev, P.; English, N. J.; MacElroy, J. M. D. Molecular dynamics study of water in contact with the TiO 2 rutile-110, 100, 101, 001 and anatase-101, 001 surface. Mol. Phys. 2011, 109, 1649–1656 DOI: 10.1080/00268976.2011.582051.
45. Liu, L.-M.; Zhang, C.; Thornton, G.; Michaelides, A. Structure and dynamics of liquid water on rutile TiO_2 (110). Phys. Rev. B 2010, 82, 161415(1–4) DOI: 10.1103/PhysRevB.82.161415.
46. Skelton, A. A.; Liang, T.; Walsh, T. R. Interplay of Sequence, Conformation, and Binding at the Peptide−Titania Interface as Mediated by Water. ACS Appl. Mater. Interfaces 2009, 1, 1482–1491 DOI: 10.1021/am9001666.
47. Schneider, J.; Colombi Ciacchi, L. Specific Material Recognition by Small Peptides Mediated by the Interfacial Solvent Structure. J. Am. Chem. Soc. 2012, 134, 2407–2413 DOI: 10.1021/ja210744g.
48. Momma, K.; Izumi, F. VESTA: A Three-Dimensional Visualization System for Electronic and Structural Analysis; 2014.

49. Hanggi, P.; Talkner, P.; Borkovec, M. Reaction-Rate Theory: Fifty Years after Kramers. Rev. Mod. Phys. 1990, 62, 251–342 DOI: 10.1103/RevModPhys.62.251.

TOC Graphic

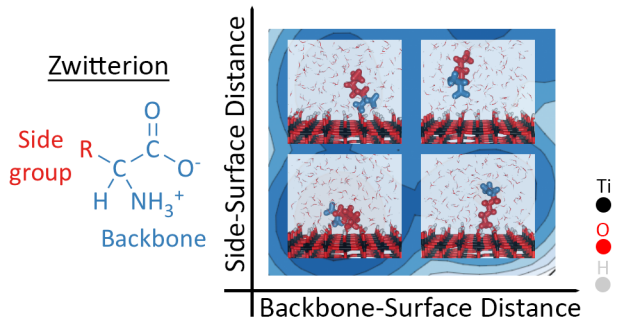
Zwitterion
Side group
R
C
O
O⁻
H
NH3+
Backbone
Side-Surface Distance
Backbone-Surface Distance
Ti
O
H